TU Delft

Delft University of Technology

Document Version
Final published version

Citation (APA)
Karaoulis, M., Diamanti, N., Bremmer, C., Slob, E., Ngan-Tillard, D., & Karamitopoulos, P. (2025). Application of Ground Penetrating Radar and Electrical Resistivity Tomography for Recognizing Cavities in Critical Urban Areas: The Case Study of Muntplein (Amsterdam, the Netherlands). In N. Diamanti (Ed.), *13th International Workshop on Advanced Ground Penetrating Radar, IWAGPR 2025 - Proceedings* IEEE. https://doi.org/10.1109/IWAGPR65621.2025.11109010

Important note
To cite this publication, please use the final published version (if applicable).
Please check the document version above.

Copyright
In case the licence states “Dutch Copyright Act (Article 25fa)”, this publication was made available Green Open Access via the TU Delft Institutional Repository pursuant to Dutch Copyright Act (Article 25fa, the Taverne amendment). This provision does not affect copyright ownership.
Unless copyright is transferred by contract or statute, it remains with the copyright holder.

Sharing and reuse
Other than for strictly personal use, it is not permitted to download, forward or distribute the text or part of it, without the consent of the author(s) and/or copyright holder(s), unless the work is under an open content license such as Creative Commons.

Takedown policy
Please contact us and provide details if you believe this document breaches copyrights.
We will remove access to the work immediately and investigate your claim.

This work is downloaded from Delft University of Technology.

Green Open Access added to TU Delft Institutional Repository
as part of the Taverne amendment.

More information about this copyright law amendment
can be found at https://www.openaccess.nl.

Otherwise as indicated in the copyright section:
the publisher is the copyright holder of this work and the
author uses the Dutch legislation to make this work public.

Application of ground penetrating radar and electrical resistivity tomography for recognizing cavities in critical urban areas: the case study of Muntplein (Amsterdam, The Netherlands)

Marios Karaoulis
Department of Geophysics
Aristotle University of Thessaloniki
Thessaloniki, Greece
mkaraoulis@geo.auth.gr

Nectaria Diamanti
Department of Geophysics
Aristotle University of Thessaloniki
Thessaloniki, Greece
ndiamant@geo.auth.gr

Chris Bremmer
Deltares, Departmetn of Applied Geology and Geophysics
Utrecht, The Netherlands
Chris.Bremmer@deltares.nl

Evert Slob
Department of Geosciences and Engineering
Delft University of Technology
Delft, The Netherlands
E.C.Slob@tudelft.nl

Dominique Ngan-Tillard
Department of Geosciences and Engineering
Delft University of Technology
Delft, the Netherlands
d.j.m.ngan-tillard@tudelft.nl

Pantelis Karamitopoulos
Ingenieursbureau Gemeente Amsterdam
Amsterdam, The Netherlands
p.karamitopoulos@amsterdam.nl

2025 13th International Workshop on Advanced Ground Penetrating Radar (IWAGPR) | 979-8-3315-2335-0/25/$31.00 ©2025 IEEE | DOI: 10.1109/IWAGPR65621.2025.11109010

***Abstract*— Large areas behind the historic quay walls and bridges in Amsterdam city center are prone to soil mobilization and cavity (sinkhole) formation due to intensified infrastructure developments and extreme groundwater level fluctuations caused by climate change. We carried out a geophysical survey to investigate a sinkhole formed under the Muntplein (Amsterdam, The Netherlands). The surface trace (hole) of the sinkhole was triggered by a heavy vehicle passing over the street which lies in the vicinity of a quay wall and behind the abutment of the Muntsluis bridge. The application of ground penetrating radar (GPR) and electric resistivity tomography (ERT) provided continuous data of the shallow subsurface which enabled the detection of the backfilled cavity, its southwest (SW) extension, the bridge abutment-to-soil transition, key utility lines and the presence of two potential targets for further investigation. A follow-up geotechnical assessment supported by hydrographic survey in the canal validated our findings and substantiated our first interpretation (i.e., sinkhole in development). The paper demonstrates the applicability of non-invasive electromagnetic (EM) methods to rapidly detect cavities in critical urban areas, and, thus, to de-risk climate-smart infrastructure developments.**

Keywords—near-surface geophysics, GPR, ERT, human-induced sinkhole, quay wall, electromagnetic sensing, smart and climate resilient cities

I. Introduction

Non-invasive geophysical methods are becoming increasingly important to the planning of future infrastructure developments and smart city programs [1]. The city of Amsterdam has been a major player against global warming and the implementation of innovative climate-smart projects in favour of sustainable economic development (http://www.citego.org/bdf_fiche-document-883_en.html). However the adaptation of the city's surface and unconsolidated shallow subsurface to a water system that is very close to sea level, led to persistent subsidence imposing additional risks to city infrastructure related to ground instability phenomena [2].

A significant proportion of ground instability phenomena (in urban areas) is ascribed to the development of sinkholes induced by various anthropogenic activities. Sinkholes may form slowly without noticeable traces or suddenly when a collapse occurs leading to hazardous effects in urban settings.

While in-situ geotechnical investigations (e.g. borehole drilling, cone penetration tests, pit excavations) may yield hydrological and mechanical properties of the soils surrounding quay wall structures, they provide limited information about the 2-D and 3-D spatial distribution and internal heterogeneity of the soils or the presence of hazardous cavities (sinkholes). Due to the absence of time-lapse information, the genetic mechanisms responsible for the cavity/sinkhole formation behind quay wall structures are rarely quantified. Furthermore, data fusion i.e., the integration of existing and newly acquired data to provide complementary information on subsoil conditions, is rarely implemented.

Non-invasive geophysical surveying provides the means to obtain continuous 2-D and 3-D data in a fast, safe, cost-effective and repeated manner and thus capture 3-D subsoil heterogeneity and cavity formation [3], [4].

II. Background & Methods

A. Survey area

On January 4, 2021, a cavity developed on the road surface near Munplein in Amsterdam (Fig. 1). The hole was created when a vehicle passed by but the subsurface extent of the cavity under this hole revealed that it has been present for some time given its nature and size. The municipality of Amsterdam is currently working on a comprehensive program to repair quay walls and bridges. Quays instabilities could be also attributed to heavy traffic in the canals, additional load on structures due to waves, scouring by engines, dredging to allow navigation, etc. [5]. During a preliminary investigation, the suspicion arose that there might be more cavities at the level of the bridges and quays.

Authorized licensed use limited to: TU Delft Library. Downloaded on September 23,2025 at 11:27:48 UTC from IEEE Xplore. Restrictions apply.



Fig. 1. Photo of the sinkhole found on January 4, 2021 near Muntplein.



Fig. 2. GPR survey location layout on top of a utility map, carried out with a pulseEKKO PRO system. C1 to C4: corners of the GPR grid. C1C4: baseline of GPR survey, C2C3: end line. Thin blue lines: 1000 MHz GPR lines. Thick green lines: 500 MHz GPR lines. Thick black lines: street island and pavement.

B. Ground Penetrating Radar (GPR) survey

We carried out a GPR survey in the area of interest using a pulseEKKO PRO GPR in a SmartTow configuration. The pulseEKKO system series provides a wide-range of operating centre frequencies for various applications ranging from deep mineral exploration and glaciology to high-resolution geotechnical investigations and concrete imaging. One of the aims of a GPR survey is to map contrasts in the subsurface electromagnetic (EM) properties (electrical storage capacity, magnetic permeability, electrical conductivity). The EM properties of the subsurface are a function of the material type, moisture and fluid salinity if it contains fluids. Thus, a GPR survey can highlight heterogeneities in the subsurface such as empty or poorly backfilled cavities, utilities and underground infrastructure structures.

The survey took place on January 22, 2021 on a dry day after a week of heavy rain. The main part of the survey consisted of acquiring GPR data in the constant offset mode with 1000 MHz center frequency (f_c) antennas across a grid (Fig. 2). The grid was made up of lines with 0.15 m spacing, marked on the ground with a nylon rope. The small line spacing is adapted to the footprint of the 1000 MHz f_c antennas and allows for effective interpolation between lines. Even though the targeted sinkholes are large (from several decimeters to a few meters), a good lateral resolution is needed to pick up smaller anomalies like sand erosion channels, image transition zones to the sinkholes and position sinkholes with respect to neighbouring utility lines or line infrastructures. Data was recorded along the lines in a zigzag mode meaning that after collecting a line from start to end, the next, neighbouring line was collected from end to start, primarily to save time during data acquisition.

The spatial sampling along the lines was set at 0.01 m using odometer triggering for the GPR transmitter. The recording time window was set to 35 ns. To ensure sufficient signal-to-noise ratio of the recordings along all lines and at the same time allow for a practical data acquisition speed without skipping traces, the number of stacks at each recording point was set to 8. Using the 1000 MHz f_c transducers provided high resolution, enabling the imaging of the uppermost part of the road structure, where sinkholes are close to outcropping on the road surface.

Three additional lines were recorded also in the constant offset mode using the 500 MHz f_c antennas and parallel to the electrical resistivity tomography (ERT) lines (that will be described in a later section): one line on the zebra crossing – outside the sunk road surface, one line across the sunk surface and a third one on the street island, crossing a zone below which an extension of the proven sinkhole is expected (Fig. 2). In this study, we have focused on the grid data collected with the 1000 MHz center frequency transducers.

C. Electrical Resistivty Tomography (ERT) survey

A typical acquisition system for DC (direct current) resistivity measurements consists of a resistivity meter, an electrical source (battery), cables with electrodes, a switch cabinet and a control and storage unit (computer). For each measurement, two current electrodes are used: one to inject the current into the subsurface and the other to extract the same amount of current from it. By convention, these electrodes are called A and B, respectively. The electric field is measured (at least) with two other electrodes (M and N), the potential electrodes. The way in which the current and potential electrodes are arranged on the earth's surface is called an array. By changing the configurations of the array, the properties of the subsurface are mapped. A large number of electrode arrays have been designed, using different electrode positions along a profile. By using switch cabinets, it is possible to perform a large number of measurements in a short time, which makes it possible to repeat measurements over longer periods (time-lapse data). These systems are capable of collecting data with high spatial resolution, allowing for better and more reliable tomographic results. We used the system MPT DAS-1 (Fig. 3) that has an 800 V transmitter and can inject up to 2 A of current. More information can be found by Revil et al. [6].

We measured a set of six (6) ERT lines with twenty-one (21) electrodes per line, as shown in Fig. 3. Electrode spacing was set to 1 m along the line and 1.5 m between the lines. In order to cover the entire survey area, this configuration was shifted five (5) lines after each set of measurements, where Line 6 of the previous measurement set became Line 1 of the new set. In total, measurements were taken along fourteen (14) lines. This type of measurement setup and subsequent processing allowed for 3D data interpretation. The complete dataset consisted of 4,573 measurements.

Authorized licensed use limited to: TU Delft Library. Downloaded on September 23,2025 at 11:27:48 UTC from IEEE Xplore. Restrictions apply.

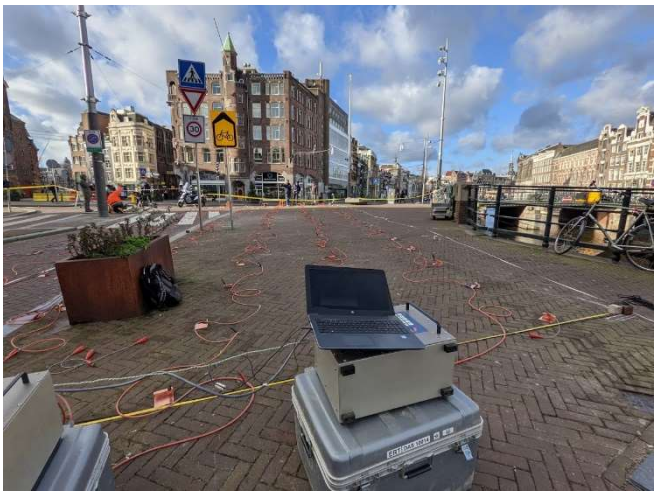


Fig. 3. ERT survey at Muntplein using the MPT DAS-1 system.

III. Data Processing & Results

A. GPR data

We used the EKKO_Project software to process the data. As GPR measures travel times and amplitudes of reflections, to convert these travel times to a depth range, we used an average velocity for GPR signals in the subsurface of 0.085 m/ns, which was estimated by hyperbola fitting. The main processing procedure applied to GPR profiles was (a) time zero adjustment, (b) various functions of time gain to compensate the signal attenuation with depth and (c) frequency filtering, for the elimination of undesirable frequencies. Since the GPR data were measured in a grid mode, by combing all GPR profiles we were able to produce maps of the subsurface at various times or equivalent depths (i.e., time or depth slices). For the construction of GPR depth slices, further processing was necessary in order to enlighten anomalies due to local inhomogeneities, such as background subtraction, trace envelope and migration.

Fig. 4 illustrates selected depth slices for the survey area. The surface depth slice (less than 0.1 m depth), shows the street layout clearly the as it is associated to differences in construction material properties and sharp surface elevation differences (Fig. 4a). Among others, linear features such as the zebra crossing, the marble line, the pavement curbs along Amstel and the street island are clearly visible., These features remain noticeable even in later time slices (as the time shifts persist in the recordings) and are used as "landmarks" to orient ourselves on the time-slices maps.

The location of the shallow backfilled sinkhole under the zebra crossing of the northern Amstel lane is clearly delineated on the depth slice at ~0.20 m (Fig. 4b). The strong reflections, marked with a solid circle, are associated to the reflections from the surface slabs / sinkhole interface, also indicated by an arrow on one of the corresponding radargrams. Both the main sinkhole and its extension are associated to the area with no reflections below the aforementioned interface. Reflections beneath the main sinkhole are attenuated due to the lossy nature of the backfilling material. This backfilled main sinkhole is quasi circular and has a diameter between 2.3 and 2.7 m. A portion of the sinkhole is located under the central part of the street island. The responses related to the main sinkhole extension under the street island (annotated with dashed circle and dashed line on the depth slice and cross section, respectively of Fig. 4b), do not suffer from signals' attenuation, as complete backfilling has not taken place in the area.

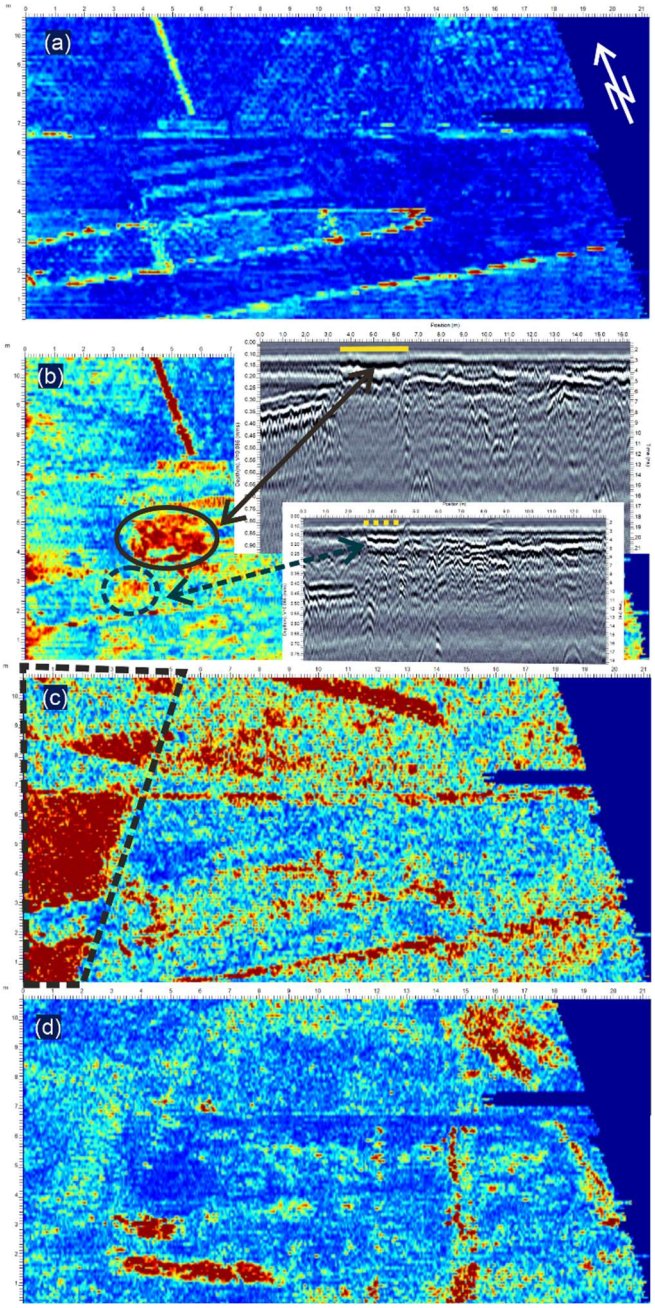


Fig. 4. Depth slices for the GPR survey at various depths: (a) surface depth slice – less than 0.1 m, (b) ~0.20 m, (c) 0.60 m and (d) 0.90 m. Warm colors (red) indicate areas of increased reflectivity and cold colors (blue) indicate quiter areas in terms of reflectivity. In (b) two radargrams have been added to indicate (i) the location of the sinkhole (annotated with a solid circle on the depth slice and a solid yellow line on the cross section) as well as (ii) the location of the sinkhole extension towards the southwest (annotated with a dashed circle on the depth slice and a dashed yellow line on the cross section). In (c) a trapezoidal zone of increased reflectivity is annotated with a dashed polyline. This zone is due to the presence of the deck and east wall of the Muntsluijs.

In Fig. 4c, a trapezoidal zone on the eastern side of the grid is seen. The superposition of the GPR time slices onto the utility map indicates that the anomaly is likely to represent the deck and east wall of the Muntsluijs. The structure dips, unevenly to the west. It is adjacent to the proven sinkhole. Its northern part comes out at later times due to height differences of the street topography.

Authorized licensed use limited to: TU Delft Library. Downloaded on September 23,2025 at 11:27:48 UTC from IEEE Xplore. Restrictions apply.

Finally, regarding the depth slices of Fig. 4, several utilities were identified (i.e., linear features in warm colors) up to almost 1 m depth. Some of these linear features coincide with subsurface utilities indicated on the utility map of Fig. 2, while more linears were mapped with GPR which were not known a priori and therefore, not included in the utility map.

B. ERT data

The ERT processing software PyGIMLi [7] was used to process the data. During data processing, combinations of electrodes along each measurement row (in-line measurements) and combinations of electrodes between adjacent measurement rows (cross-line measurements) were performed. A typical workflow uses the raw data to eliminate electrodes with high contact resistances. We used flat electrodes on top of rocks, gelling the electrode contacts to improve contact resistance and therefore, no electrodes were removed from the data set. The ERT data were then filtered for the so-called 'misfits'. After this quality analysis, the final data set consisted of 4188 data points (in other words, only 9% of the data points had a higher misfit that we removed due to noise). The software converged to a solution after 6 iterations with an RMS error of 13.5%. A typical RMS error for soil conditions is around 5%, so given the conditions, the data are considered to be of high quality.

Similarly to GPR, as the ERT data were collected on a grid, all ERT lines were combined and properly processed to produce depth slices of the survey area at various depths, as illustrated in Fig. 5. More specifically, in Fig. 5a (~0.20 m depth) there is a clear wedge with high electrical resistivity visible in the northeastern corner of the study area. This is the Muntsluis and the abutment responses which correspond to the existing stone construction (abutment) and the absence of soil and water behind the abutment. Also, on the north side of the depth slice, a zone with a high electrical resistivity can be clearly seen. This corresponds to the location of a transformer cellar and a bundle of electricity and data cables located there. Also, the existing sinkhole is clearly seen, with low electrical resistivity. This was not expected beforehand because it was assumed that an empty space (void) would have a high electrical resistivity. However, since the sinkhole was filled with soil which was extra moist due to the increased precipitation during the week before data collection, the low resistivity values are justified.

In addition, in Fig. 5 we have added a GPR slice at ~0.20 m depth in an attempt to correlate the results from ERT and GPR data. As seen, the location of the existing sinkhole is clearly identified with both methods. Also, two additional locations for possible sinkholes have been identified with ERT data while only one of them has been possibly located with GPR.

It should be noted that the GPR slice at ~ 0.20 m depth, shows strong reflections where the sinkhole is located. This initially appears contradictory to the ERT data which indicate increased electrical conductivity at this location. However, for GPR, these reflections do not originate from the sinkhole itself but rather from the surface slabs / sinkhole interface. As seen in the corresponding radargrams, the sinkhole area itself appears as a reflection-free zone due to increased attenuation caused by the backfilling material. Thus, despite seeming contradictory at first glance, the results of the two methods are in agreement.

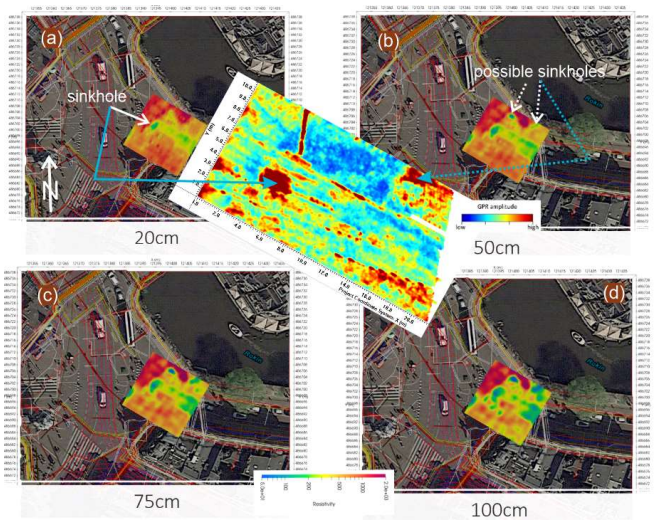


Fig. 5. Inverted resistivity results illustrating depth slices produced by ERT measurements: (a) 0.2 m, (b) 0.5 m, (c) 0.7 m and d) 1.0 m. A white solid arrow indicates the location of the known sinkhole. Two more locations of possible sinkholes were derived from ERT data (dashed white arrows). A GPR depth slice has been also added (~0.20 m) in an attempt to correlate ERT and GPR data (i.e., sinkhole and possible sinkhole locations –blue solid and blue dashed arrows, respectively).

IV. Summary & Conclusions

The combined application of ERT and GPR appeared to be valuable in studying the Muntplein subsurface in Amsterdam for sinkhole locating. The ERT measurements provided an initial estimate on the location of anomalies that may be related to sinkhole investigation and also, a sufficiently large depth range for the application in question. GPR, being a high resolution method, is appropriate for sinkhole detection in the near subsurface.

The main points of the current study are summarised below:

- Various street elements could be recognised on the shallowest GPR depth slice, such as curbs, the traffic island, zebra stripes and the pavement tiles for guiding the visually impaired.
- Both the ERT and GPR measurements showed the abutment of the Muntsluis response. The abutment runs diagonally across the area under investigation on the northwest side and can be seen in the ERT measurements as an area with high electrical resistivity and in the ground radar images as an area with high amplitudes in radar reflections.
- In the images from both methods, an anomalous zone is found just south of the transformer cellar, related to the presence of a casing with a bunch of cables and pipes. This is related to strong reflections in the ground radar measurements and an area with high electrical resistivity in the ERT images. As the GPR method has a much higher lateral and vertical resolution that the ERT method, individual utilities, such as pipes and cables, were located with GPR in great detail for the whole survey area. Some of them were known and annotated on the utility map however, there were more that were located with GPR, their presence being previously unknown.
- The location of the known sinkhole structure was easily tracked in the radargrams as well as its extension to the

Authorized licensed use limited to: TU Delft Library. Downloaded on September 23,2025 at 11:27:48 UTC from IEEE Xplore. Restrictions apply.

SW. The ERT method also identified the existing sinkhole structure. The reduction in electrical resistivity in the ERT measurements at the sinkhole location is explained by the presence of wet soil with which the hole was filled.

- From the ERT measurements we could identify two anomalies similar in response type and depth range to the one observed at the location of the existing sinkhole (i.e., Fig. 5b – dashed white arrows). The GPR results seem to identify one location of a possible sinkhole (i.e., Fig. 5b – dashed blue arrow) and not two like the ERT method.
- It should be noted that for GPR and ERT methods, a direct depth comparison of the targets' exact location may be misleading. This is due to the fact that the two methods have resolution and sensitivity differences – GPR has a higher resolution than ERT, while the latter method typically penetrates deeper than GPR but with a lower resolution both in depth and laterally.

ACKNOWLEDGMENT

We would like to thank Gemeente Amsterdam Ingenieursbureau T.a.v. and more specifically, Ms R. van Schooneveld.

REFERENCES

[1] R. K. Bellanova, Lindskov Jacobsen, and L. Monsees, "Taking the trouble: Science, technology and security studies," Critical Studies on Security 8 (2): 87–100, 2020. doi:10.1080/21624887.2020.1839852.

[2] J. Schokker, M.A.J. Bakker, C.W. Dubelaar, R.M. Dambrink and R. Harting, "3D subsurface modelling reveals the shallow geology of Amsterdam. Netherlands," Journal of Geosciences, 94, pp 399-417, 2015. doi:10.1017/njg.2015.22 .

[3] D. Gómez-Ortiz, and T. Martín-Crespo, "Assessing the risk of subsidence of a sinkhole collapse using ground penetrating radar and electrical resistivity tomography," Engineering Geology 149-150, 1-12, 2012.

[4] G. Vargemezis, P. Tsourlos, I. Fikos, N. Diamanti, D. Angelis, and E. Amanatidou, "Void Detection and Consolidation Filling Verification by ERT, GPR and Seismic Refraction Methods," Near Surface Geoscience 2019, 5 pp., The Hague, The Netherlands, 2019.

[5] M. J. Profittlich, F. C. M. Seignette, R. Rozing, and C. Kroon, "Investigation into cause of quay wall failure: Quay wall Grimburgwal Amsterdam," Fugro Report, 2720-175666.R01 V03, in Dutch, 2020.

[6] A. Revil, M. Karaoulis, T. Johnson, and A. Kemna, Review: Some low-frequency electrical methods for subsurface characterization and monitoring in hydrogeology. [Revue: Méthodes électriques basses-fréquences et leurs applications à la caractérisation du sous-sol et au suivi hydrogéologique] Hydrogeology Journal 20 (4), 617-658, 2012. doi:https://doi.org/10.1007/s10040-011-0819-x.

[7] C. Rücker, T. Günther, F. M. Wagner, pyGIMLi: An open-source library for modelling and inversion in geophysics, Computers and Geosciences, 109, 106-123, 2017. doi: 10.1016/j.cageo.2017.07.011.

Authorized licensed use limited to: TU Delft Library. Downloaded on September 23,2025 at 11:27:48 UTC from IEEE Xplore. Restrictions apply.